Journal of the European Ceramic Society **16** (1996) 133–141

0955-2219(95)00141-1 0955-2219/96/$15.00

Anisotropic Grain Growth in Seeded and B_2O_3-doped Diphasic Mullite Gels

S.-H. Hong, W. Cermignani & G. L. Messing

Department of Materials Science and Engineering, The Pennsylvania State University, University Park, PA 16802, USA

(Accepted 22 July 1995)

Abstract

Anisotropic grain growth in mullite was investigated in B_2O_3-doped diphasic gels seeded with either mullite particles or whiskers. Anisotropic grain growth was observed in all systems. The largest anisotropic grains were obtained with a system seeded with 2 wt% mullite whiskers and doped with 2 wt% B_2O_3. The mullite whiskers act as sites for multiple nucleation and subsequently as templates for mullite overgrowth. Boria lowered the mullite formation temperature by 150°C and it significantly enhanced anisotropic grain growth independent of the presence of seed particles. This enhancement was attributed to increased dissolution of alumina.

1 Introduction

Anisotropic grain growth is one class of *in situ* reaction that is relatively unexplored but appears to offer significant opportunity for the development of new materials with self-reinforcing microstructures. Silicon nitride (Si_3N_4) is exemplary of how the mechanical properties of a polycrystalline ceramic can be improved by optimizing grain growth of anisotropic β-silicon nitride grains during the α to β-Si_3N_4 phase transformation. Today, silicon nitrides with fracture toughnesses of 10–20 MPa $m^{1/2}$ can be routinely produced. Such highly fracture-resistant materials are a result of extensive experimentation. There is surprisingly little fundamental understanding about the processes leading to growth of anisotropic grains. Although silicon nitride has excellent mechanical characteristics, its low oxidation resistance limits its use in high temperature applications. Clearly, there is a need for oxide ceramics having similar self-reinforcing microstructures.

Mullite ($3Al_2O_3{\cdot}2SiO_2$) has been recognised as an important structural and optical material due to its excellent high temperature strength, creep resistance, good chemical and thermal stability, low thermal expansion coefficient and infrared transparency.[1–3] The stable crystal structure of mullite is orthorhombic with lattice parameters a = 7·5456 Å, b = 7·6898 Å and c = 2·8842 Å (JCPDS Card # 15–776), and is composed of octahedral AlO_6 chains aligned in the c-direction and crosslinked by corner-shared AlO_4 and SiO_4 tetrahedra.[4] Thus, unrestricted growth parallel to the c-axis favours the development of anisotropic grains.

A number of authors have demonstrated that sol–gel processes can be designed to control the degree of alumina–silica mixing and, consequently, control mullite crystallization kinetics, densification and microstructure evolution.[5] Several authors[6–10] have studied microstructural development of aluminosilicates with compositions near the single-phase mullite region. Equiaxed grains in alumina-rich mullites have been attributed to the kinetic limitation of material transport by solid-state diffusion whereas the presence of a liquid phase has been suggested to facilitate the growth of anisotropic grains in silica-rich mullites (i.e. < 74 wt% Al_2O_3). While a sol–gel polymeric mixture resulted in the equiaxed microstructure, variations in local chemical heterogeneity in a sol–gel colloidal mixture lead to anisotropic mullite grains at the same composition (72 wt% Al_2O_3).[5]

In ceramic systems which transform by nucleation and growth, another way to control microstructure evolution is to seed the precursor material. A homogeneous, fine-grained matrix ceramic can be obtained by using seed concentrations > 10^{13} seed particles/cm^3 of matrix material. Huling and Messing[11] demonstrated that a fully dense, nominally 0·2 μm grain size mullite was obtained by seeding a diphasic gel with 30 wt% polymeric gels. They also reported that a hybrid gel consisting of polymeric and diphasic gels could be designed to control the nucleation frequency, reduce the grain size, and increase the microstructural homogeneity in a manner analogous to particle seeding. Mroz and Laughner[12] utilized

seeding to enhance anisotropic grain growth of mullite and reported that a dense, equiaxed grain structure was developed at a relatively high seed concentration, whereas highly anisotropic, large grains dispersed in a matrix of small, equiaxed grains were obtained at a low seed concentration.

Important factors affecting grain growth processes are: (1) the grain size of the microstructure when the sintered products become fully dense, and able to support grain growth (i.e. free of boundary inhibiting pores); and (2) the transport rate and solubility in systems with liquid phases. A dense, fine-grain microstructure has a large surface free energy associated with the grain boundaries and, thus, a large driving force for grain growth. The importance of a fine initial microstructure for anisotropic grain growth was recently demonstrated in TiO_2-doped alumina obtained by seeding an alumina gel.[13]

In the mullite system, it is known that densification is aided by viscous flow of the amorphous silica phase and that this glass phase also enhances the development of anisotropic grains. The viscosity of the glass phase in mullite can be decreased by several orders of magnitude by adding glass-forming oxides such as boron oxide (B_2O_3) and phosphorous oxide (P_2O_5). Na_2O, which is known to lower the viscosity of silica glasses, did not enhance either the mullite crystallization kinetics or the densification rate.[14] However, the grain size increased and grain morphology changed from equiaxed to anisotropic with increasing Na_2O concentration. When B_2O_3 was added to a mullite precursor, it was reported to react first with alumina to form aluminum borate, $9Al_2O_3{\cdot}2B_2O_3$, a stable crystalline compound,[15] and then to form the mullite phase. Thus, B_2O_3 significantly decreased the temperature of mullite formation.

The crystal structure of aluminum borate ($9Al_2O_3{\cdot}2B_2O_3$) is orthorhombic, it has lattice parameters a = 7·6874(8) Å, b = 15·0127(5) Å and c = 5·6643(6) Å (JCPDS Card # 32-3) and it consists of AlO_6 octahedra, AlO_4 tetrahedra, AlO_5 coordination polyhedra and B_2O_3 triangles.[16] Based on similarities in the crystal structure and lattice parameters, it is reasonable to propose that aluminum borate can act as an epitaxial substrate for mullite nucleation and growth. Based on transmission electron microscope analysis, Richards *et al.* reported that the glass-forming oxides such as B_2O_3 or P_2O_5 do not exist as free glassy phases at the grain boundaries in sol–gel derived mullite fibres.[17]

While anisotropic grains are often observed in mullite ceramics, there have been few attempts to develop a self-reinforcing mullite microstructure. Also, it is not well understood how boria affects the mullite transformation kinetics and microstructural development. In this paper, we report a series of experiments designed to learn how the initial microstructure and the grain boundary chemistry can be adjusted to obtain a self-reinforced mullite microstructure. The objective of these initial studies is to learn about the fundamental factors controlling anisotropic grain growth in mullite.

2 Experimental Procedure

Microstructural development was evaluated for two series of samples. The first series of samples was seeded with either mullite seed particles or mullite whiskers. Any differences between these samples can be attributed primarily to the effect of the seeds on the mullite formation and subsequent microstructure evolution. Boria was added to a second series of samples to investigate the role of phase equilibria and transport on the mullite formation and anisotropic grain growth.

The diphasic sols were prepared from boehmite [γ-AlO(OH)] powder (Catapal D, Vista Chemical Co., Houston, TX) and a silica sol (Ludox AS-40, Du Pont Co., Wilmington, DE). Additional details are described elsewhere.[11] All samples contained identical Al_2O_3/SiO_2 ratios prior to calcination and were within the single-phase mullite region (~73 wt% Al_2O_3).

A mullite seed dispersion was prepared by dispersing a commercial mullite powder (Chichibu Cement Co., Ltd, Saitama, Japan) in distilled water adjusted to pH 3 with nitric acid. The dispersion was stirred for 3 days, sonicated and centrifuged at 2000 rev min^{-1} for 30 min and the particles in suspension were used for seeding. The particle size distribution of the mullite seed particles was measured by a laser scattering technique (Horiba LA-900, Horiba Instrument Inc., Irvine, CA). The mullite whiskers (MW-10, Chichibu Cement Co. Ltd, Saitama, Japan) were dispersed in a manner similar to the mullite powder. The boria was introduced to the sol system as boric acid (H_3BO_3).

After heterocoagulating the boehmite and silica sol, they were gelled at 80°C. The gels were dried for 12 h at 80°C, ground with an alumina mortar and pestle, and sieved to < 74 m (–200 mesh). The powder was dry pressed at low pressure and then pellets, 12·7 mm diameter and 3 mm thickness, were cold isostatically pressed at 200 MPa. The pressed pellets were heated in air from 1600 to 1650°C for 1 to 10 h. For microstructure observation, the sintered samples were cut in half, polished with 0·1 μm diamond paste and thermally etched at 100°C below the sintering temperature.

The micrographs were taken near the centre of the sample. An apparent aspect ratio was measured on the polished surface, but so far we have not attempted to calculate or measure the true aspect ratio.

The mullite formation temperature was determined by differential thermal analysis (DTA) at 10°C min^{-1} in air (Thermal Analyst 2100, TA Instrument, New Castle, DE). X-ray diffraction (XRD) was used to determine the phases present after calcination, and the apparent density of the sintered samples was measured by the Archimedes method.

3 Results and Discussion

3.1 Mullite particle seeding

As determined by inductively coupled plasma emission spectroscopy (Leeman Labs PS3000UV), the composition of the mullite powder is 71·5 wt% Al_2O_3 and 28·5 wt% SiO_2. This composition is very close to that of 3:2 mullite (~71·8 wt% Al_2O_3). From the XRD measurement of the mullite powder, there was no angular separation of the reflection pair (120)/(210) around 26° 2θ, indicating that the seed particles are pseudotetragonal mullite.[18] The median particle size of the as-received powder was ~1·6 μm and the median size of the mullite seed particles was ~0·14 μm, with the size range from 0·05 to 0·4 μm. The mullite seed particles are spherical and agglomerate-free as confirmed by scanning electron microscopy (SEM).

The mullite formation temperature in the diphasic gels was determined from the DTA exothermic peak maximum. As shown in Fig. 1, the mullite formation temperature decreases from 1345 to 1330°C at 2 wt% seeding. At 10 wt% seeding, the temperature decreases to 1318°C. The ~30°C decrease in mullite formation temperature relative to the unseeded diphasic gel is comparable to earlier results by Huling and Messing.[11] With increasing particle seed concentration, the exothermic mullite formation peak broadens and is obscured by the background. Broadening of the exothermic peak with increasing seed concentration indicates that mullite formation occurs over a wide temperature range. The plateau in mullite formation temperature was shown earlier to be a result of a change in the mullite formation mechanism from nucleation control to interface reaction control.[19]

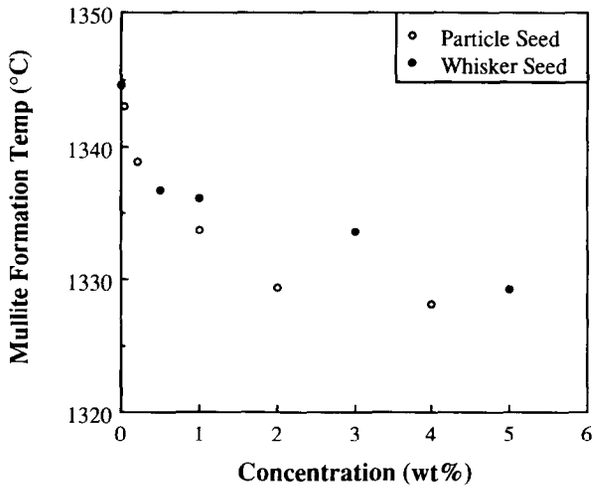

Fig. 1. Temperature of DTA exothermic peak maximum for mullite formation as a function of mullite particle and whisker concentration (heating rate: 10°C min^{-1}).

The unseeded and seeded samples were ~97% dense after sintering for 5 h at 1650°C. The microstructures of the unseeded and seeded diphasic gels sintered at 1650°C for 5 h are compared in Fig. 2. In the unseeded samples (Fig. 2(A)), most of the grains are equiaxed with a small number of anisotropic grains whose largest aspect ratio does not exceed 3. The as-received mullite powder, which was sintered at the same sintering condition, yields the same microstructure and approximately the same sintered density as the unseeded colloidal sample. The microstructure of the 0·05 wt% seeded sample (Fig. 2(B)) is similar to the unseeded sample and shows both inter- and intragranular pores. The 0·05 wt% seed concentration corresponds to ~4 × 10^{11} seed particles/cm^3 of mullite powder and is the same order of magnitude as the intrinsic nucleation density in a similar diphasic mullite system.[20] In the 2 wt% seeded sample (Fig. 2(C)), anisotropic grains with an aspect ratio of ~5–6 are distributed in a matrix of micrometre-sized grains. Most of the intragranular pores were eliminated as a result of the grain size refinement.[11] The aspect ratio in the 10 wt% seeded sample (Fig. 2(D)) does not change much relative to the 2 wt% seeding concentration, but a larger fraction of anisotropic grains was observed. The matrix grains were free of intragranular pores and were ~2 μm in size with rectangular or square shapes. The grains with the polyhedral shapes are most likely end-on views of anisotropic mullite grains.

To determine how the anisotropic grains develop, the 2 wt% seeded samples were sintered at 1600 and 1650°C for 1 to 10 h. After 5 h at 1600°C, the samples are dense with only a few intragranular pores and quite small intergranular pores. The microstructure consists of some anisotropic grains with aspect ratios between 2 and 3 in a matrix of equiaxed, micrometre-sized grains (Fig. 3(A)). A similar microstructure is observed after sintering for 1 h at 1650°C (Fig. 3(B)). Larger anisotropic grains are formed and the aspect ratio increases with increasing sintering

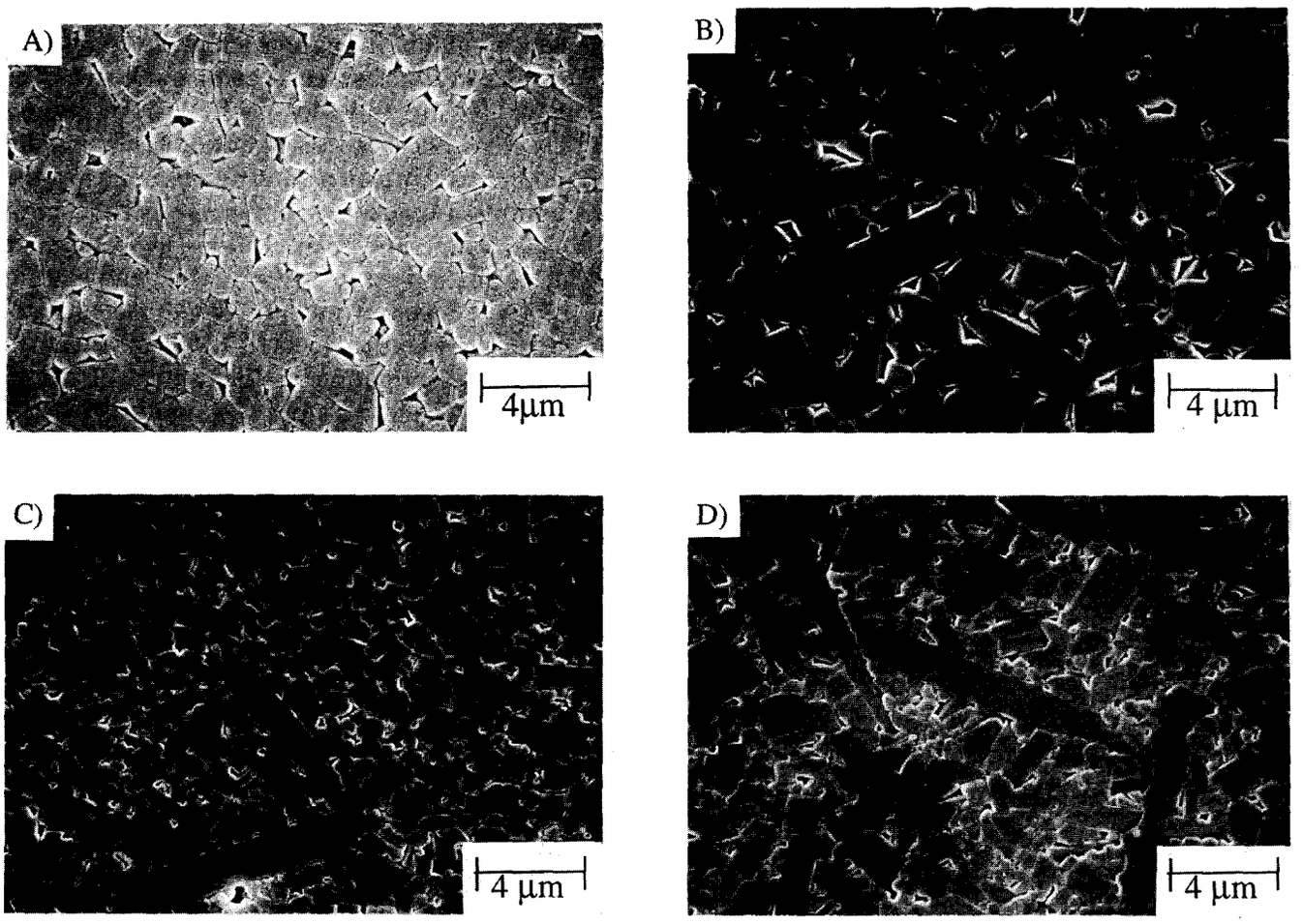

Fig. 2. SEM micrographs of polished diphasic mullite gels heated at 1650°C, 5 h. (A) unseeded; (B) 0·05 wt% mullite seeds; (C) 2 wt% mullite seeds; and (D) 10 wt% mullite seeds.

time and temperature, even though the surrounding equiaxed grains change little. This suggests that the anisotropic grains are nucleated early in the process. With increasing time and temperature, the anisotropic grains impinge and thicken to yield a microstructure of highly anisotropic grains with no intragranular pore.

The evolution of the above microstructure can be explained in terms of the driving force for grain growth and diffusion distance for pore elimination. For low or no seeding, there is a small number of mullite nuclei and grains grow from these nuclei by consuming the amorphous matrix. Thus, as pointed out earlier,[21] mullite grain boundaries sweep through a larger volume and hence, more pores during the conversion to mullite, thus leaving some of the pores isolated within the grains (Figs 2(A) and 2(B)). In the samples which were seeded above the intrinsic nucleation density, mullite seeds are the active nucleation sites, and thus reduce the grain size after complete mullite conversion. The smaller grains have a large driving force for grain growth. Some grains begin to grow at the expense of the surrounding smaller grains, and these grains become anisotropic (Fig. 2(C)). After a longer sintering time, the anisotropic grains continue to grow until they impinge. The impinged anisotropic grains cannot grow further, thus these grains begin to thicken. In highly seeded samples (Fig. 2(D)), such as 10 wt% seeding, the grains are initially much finer and the driving force for sintering and grain growth is larger than for lower seeding concentrations. Therefore, samples with a high seed concentration, sintered for a shorter time, develop a microstructure similar to samples with a lower seed concentration, but sintered for a longer time, as shown in Fig. 2(D) and in Fig. 3(D), respectively.

3.2 Mullite whisker seeding

The single crystal mullite whiskers shown in Fig. 4 have an average length of ~5 μm and a diameter of ~1 μm. The chemical composition of the mullite whisker is 73 wt% Al_2O_3; the same as that of the diphasic matrix.

The apparent density decreases slightly with increasing whisker seed concentration, and the relative density of 5 wt% whisker seeded samples sintered at 1650°C for 5 h decreased to 95%.

The mullite formation temperature decreases with increasing whisker concentration (Fig. 1). At 5 wt% whisker seed concentration, the mullite

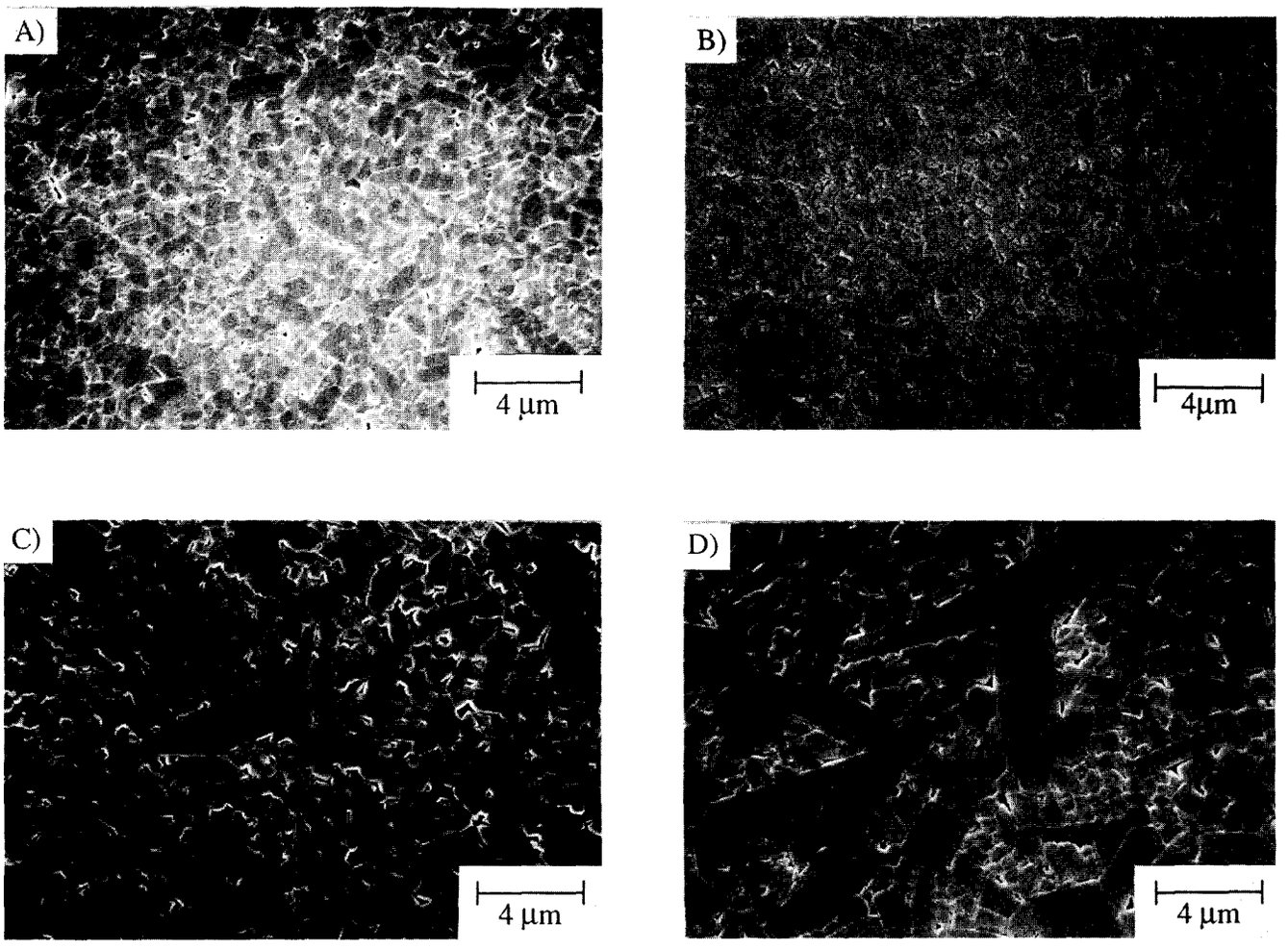

Fig. 3. Effect of time and temperature on the microstructural development of 2 wt% particle seeded mullite gels: (A) 1600°C, 5 h; (B) 1650°C, 1 h; (C) 1650°C, 5 h; and (D) 1650°C, 10 h.

formation temperature decreases by 15°C relative to that of the unseeded sample. In the whisker seeding case, the number of particles per unit weight of seeds is significantly less than in the particle seeding case but interestingly the mullite formation temperature is approximately the same. This suggests that each whisker acts as a site for multiple nucleation.

The micrographs of 1 wt% and 5 wt% whisker seeded samples sintered at 1650°C for 5 h are shown in Fig. 5. As a result of the preparation method, the whisker seeds are randomly distributed. At 1 wt% whiskers, the mullite grains appear to grow more in the axial direction rather than in the radial direction, which leads to an aspect ratio of ~8. At 5 wt% whisker concentration, many randomly distributed, anisotropic grains form and impinge to form a three-dimensionally interlocked microstructure. Again, the whiskers do not continue to grow in the axial direction, but grow in the radial direction, thus thickening the anisotropic grains and reducing the aspect ratio.

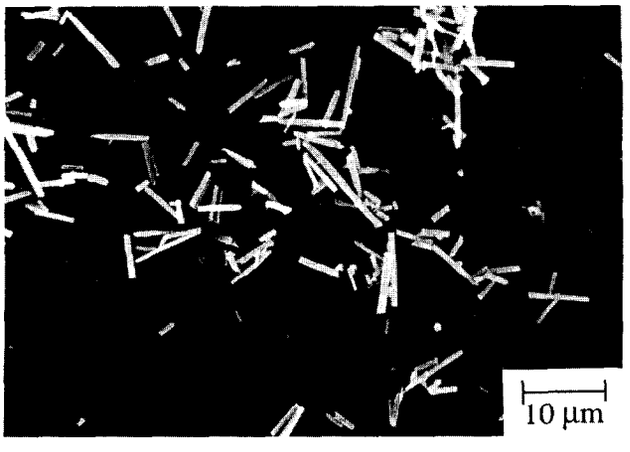

Fig. 4. SEM micrograph of single crystal mullite whiskers.

The microstructure of the 2 wt% whisker seeded colloidal mullite sample sintered at 1500°C and chemically etched with hydrofluoric acid (HF) for 15 min is shown in Fig. 6. It is evident that the whisker-shaped grain in the centre of the micrograph acted as a site for multiple nucleation. In this sample and many others observed, the anisotropic grains appear to have a mullite whisker core surrounded by an overgrowth layer as demonstrated by the presence of intragranular pores. The intragranular pores in this sample are reduced with increasing temperature and are completely eliminated at 1650°C.

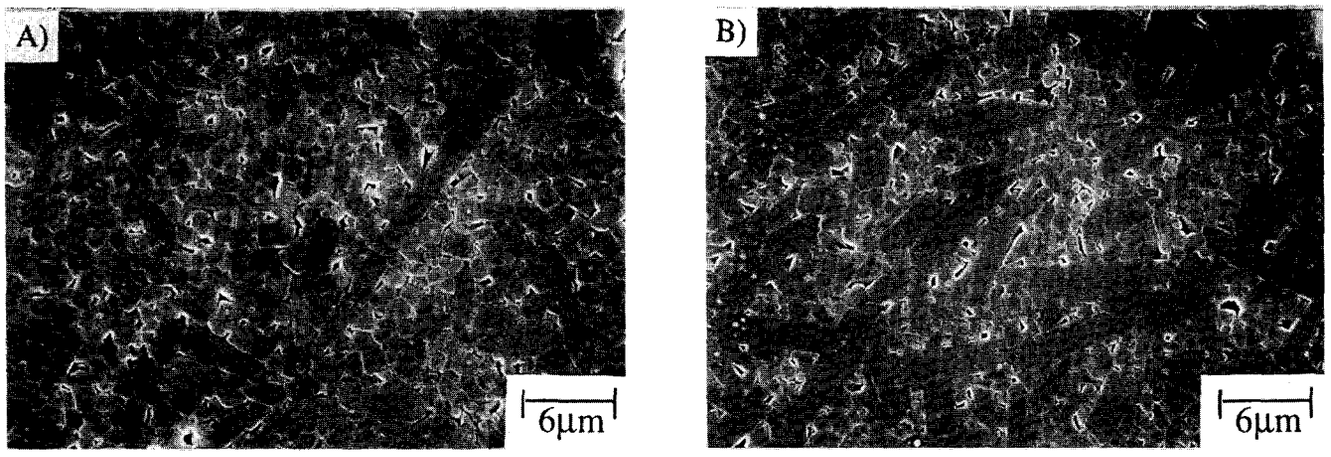

Fig. 5. SEM micrographs of mullite whisker seeded diphasic mullite gels heated at 1650°C for 5 h: (A) 1 wt% mullite whiskers; and (B) 5 wt% mullite whiskers.

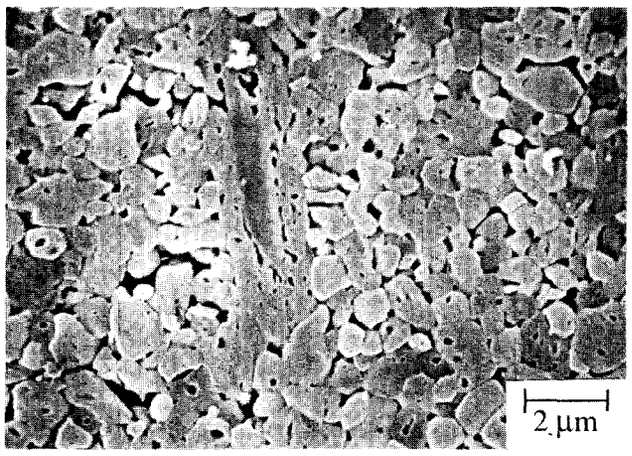

Fig. 6. SEM micrograph of chemically etched, whisker seeded diphasic mullite gel sintered at 1500°C for 5 h.

In both particle seeding and whisker seeding, the same microstructure was developed. However, seeding with whiskers allows for the possibility of aligning the elongated grains: e.g. if another forming method, such as tape casting or extrusion, is used, it is possible to develop a two-dimensionally textured microstructure.[22,23]

3.3 Boria-doped gels

As expected, the apparent density decreases with increasing boria concentration. For example, the apparent density of the 5 wt% B_2O_3-doped sample is 2·994 g cm^{-3}. The lower density may be due to the large pores surrounding the anisotropic grains as well as the lower theoretical density of B_2O_3.

Sowman[15] reported that in the Al_2O_3–B_2O_3–SiO_2 system, aluminum borate ($9Al_2O_3{\cdot}2B_2O_3$) forms first in a polymeric gel and then aluminum borosilicate crystalline phase forms by a solid solution reaction with SiO_2. He attributed the sharp exothermic peak at 885°C to the formation of an aluminum borate compound. Richards *et al.*[17] noted that this composition is not in the stable mullite phase field and contains a high B_2O_3 concentration (12·5 wt%). In 2 wt% boria-doped sol–gel derived mullite fibre, a sharp exothermic peak at 911°C was confirmed by XRD to be associated with the formation of the spinel phase, and no aluminum borate phase was detected.

In our experiments, up to 5 wt% boria was added to a diphasic gel. However, no sharp exothermic peak was observed around 885°C but a strong exothermic peak was observed between 1200 and 1350°C, which is associated with the mullite formation. No diffraction peaks for aluminum borate or aluminum borosilicate phase were detected before mullite formation, and only mullite was observed after mullite formation. A broad peak at low diffraction angles in the XRD increased with increasing boria concentration, suggesting an increase in glass content with increasing B_2O_3. The diffraction pattern of the sample sintered at 1650°C for 5 h shows an increase in (1 1 1), (1 2 1) and (3 3 1) peak intensities relative to the undoped mullite sample. This may be due to the incorporation of boron into the mullite, although this is still under investigation.

Based on chemical analysis, 60 wt% of the boria remained in the 5 wt% boria-doped sample after sintering at 1650°C for 5 h. Richards *et al.*[17] reported that after 60 h at 1400°C, 65 wt% of the B_2O_3 in their fibres volatilized. Even though our samples were sintered at higher temperature, a higher percentage of boria remained in the samples. This may be due to differences in sample dimensions and geometry. For example, the diffusion distance from the mullite fibres of Richards *et al.*[17] is significantly less than the bulk pellet samples used in this study.

The mullite formation temperature is plotted in Fig. 7 as a function of boria concentration for both unseeded and 2 wt% mullite particle seeded samples. The mullite formation temperature

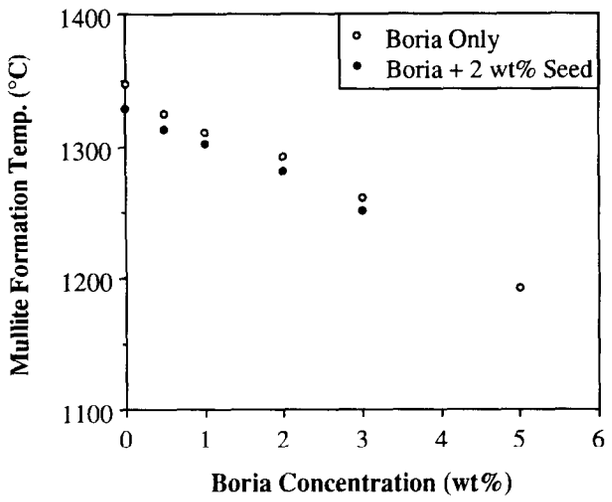

Fig. 7. Temperature of DTA exothermic peak maximum for unseeded and 2 wt% mullite particle seeded diphasic mullite gels as a function of boria addition.

decreases with increasing boria concentration for both samples. At 5 wt% boria, the mullite formation temperature decreases by 150°C relative to the undoped diphasic gel. This indicates that boria has a more dominant effect on the transformation kinetics than seeding. One possibility is that the boroaluminosilicate glass promotes mullite formation by increasing the solubility of alumina and diffusion rate in the glass phase.

Note that the microstructures of the 2 wt% particle seeded and unseeded samples are similar when B_2O_3 is present. As in the powder seeding and whisker seeding cases, the transformation peak broadened with higher boria concentrations, such that a distinct exotherm could not be observed for the 5 wt% B_2O_3, 2 wt% particle seeded sample.

Micrographs of the unseeded and 2 wt% particle seeded samples containing B_2O_3 sintered at 1650°C for 5 h are shown in Fig. 8. There is no major difference between the two samples at the same B_2O_3 concentration. In both systems, increasing the boria concentration causes the growth of highly anisotropic grains. At 5 wt% boria, most of the grains are anisotropic and their cross-sections are square or rectangular shaped. There are only a few equiaxed grains. Also, there are several intergranular pores around the anisotropic grain surfaces while there are very few intragranular pores.

3.4 Whisker seeded diphasic mullite with boria

To combine the whisker seeding and boria doping

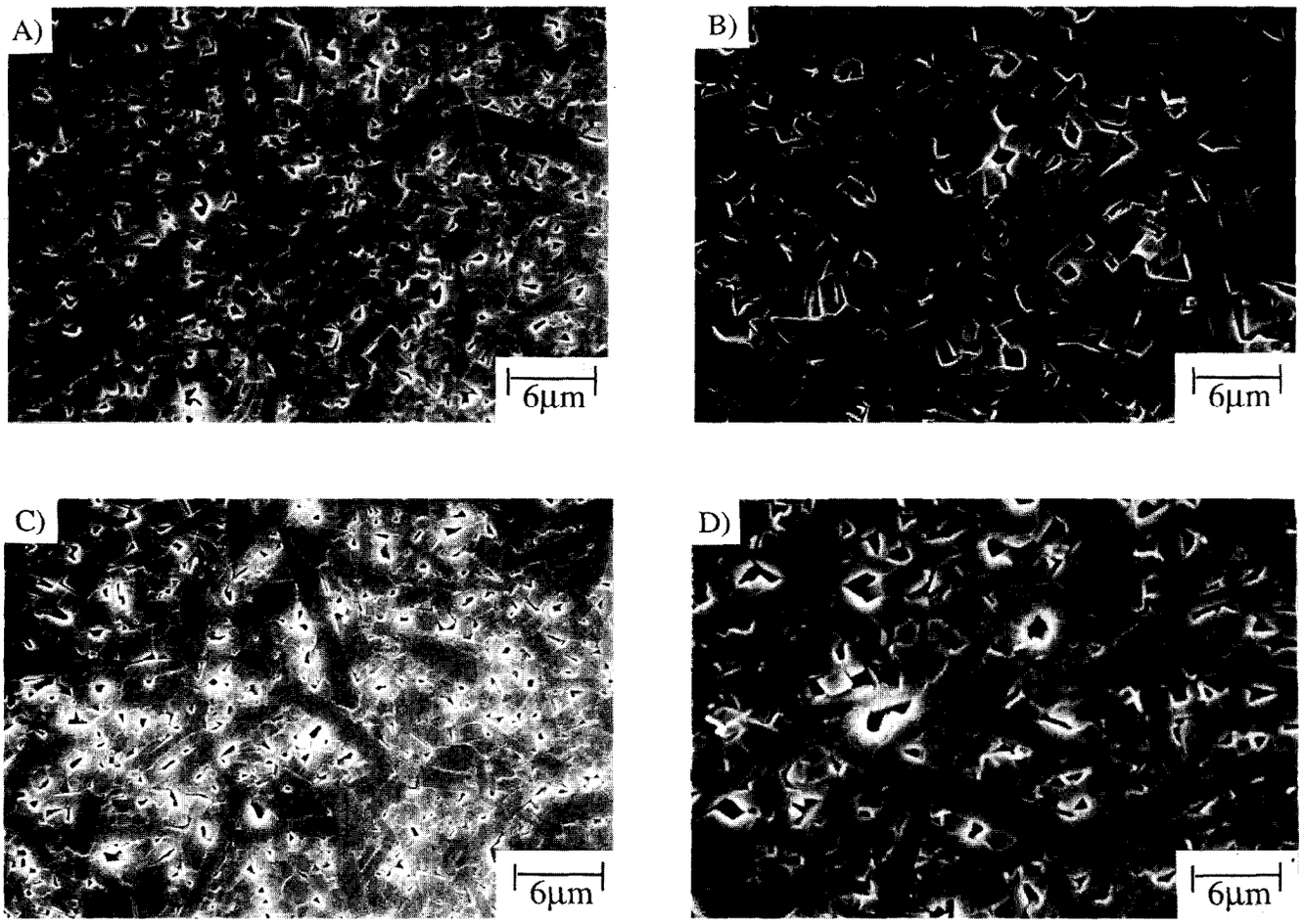

Fig. 8. SEM micrographs of samples heated at 1650°C, 5 h. Diphasic mullite gels doped with: (A) 2 wt% boria; (B) 5 wt% boria; and 2 wt% mullite particle seeded diphasic mullite doped with: (C) 2 wt% boria, (D) 5 wt% boria.

effects, 2 wt% boria was added to 2 wt% whisker seeded diphasic mullite sample. The mullite formation temperature is similar to the 2 wt% boria-doped diphasic mullite. Clearly, a microstructure of three-dimensionally interlocked, anisotropic grains is developed when this system was heated at 1650°C for 5 h (Fig. 9). Some highly anisotropic grains have an aspect ratio of >10 and a length of >30 μm.

A model for the microstructure development in whisker seeded and boria-doped diphasic mullite is shown in Fig. 10. Initially, the mullite whiskers are randomly distributed in the amorphous matrix which contains boria (stage A in Fig. 10). The single crystal whiskers provide multiple nucleation sites for overgrowth of mullite. At the same time, intrinsic nucleation occurs in the amorphous matrix (stage B). It is proposed that the boria-containing amorphous matrix facilitates the transport of diffusing ions to their preferred site along the c-axis of the whisker. Thus, the exaggerated, anisotropic grains develop by oriented overgrowth on the whiskers. At the same time, the surrounding grains are only slightly anisotropic at this stage. With further heating, a highly anisotropic microstructure is developed when the matrix grains also undergo anisotropic growth (stage C).

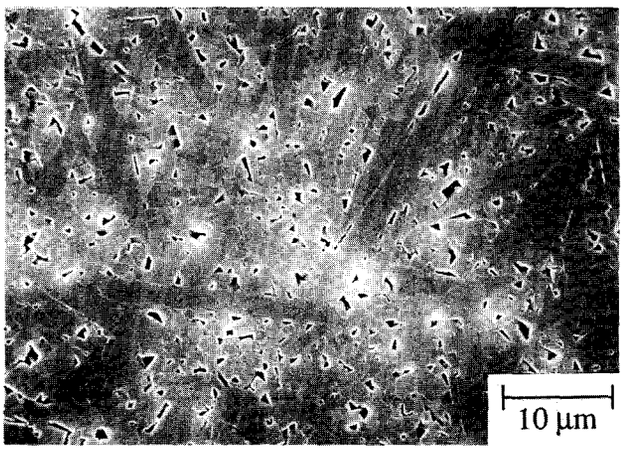

Fig. 9. SEM micrograph of 2 wt% whisker seeded and 2 wt% boria-doped diphasic mullite gel sintered at 1650°C for 5 h.

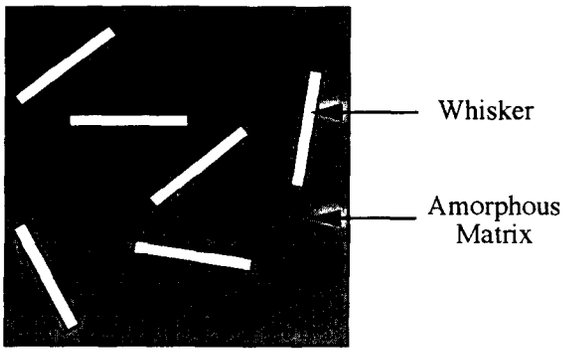

Stage A

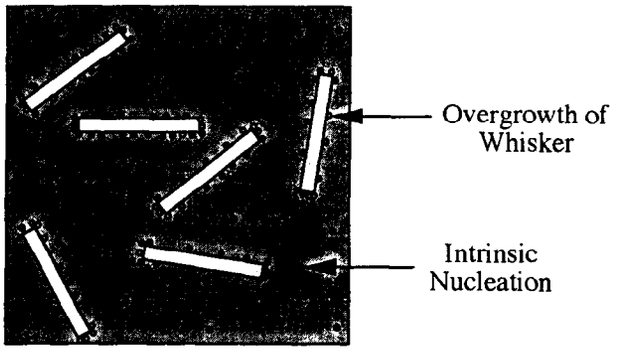

Stage B

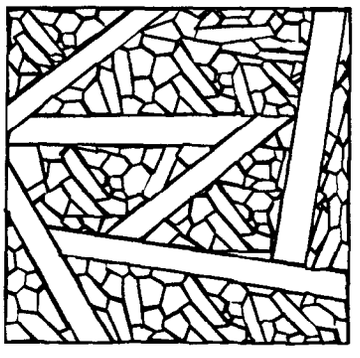

Stage C

Fig. 10. Schematic model of microstructural development in whisker seeded and boria-doped diphasic mullite gel.

4 Summary

Seeding a diphasic mullite gel with mullite particles results in a decrease in the mullite formation temperature and the development of a fine-grained microstructure. Fine grains have a large driving force for grain growth and promote the preferential growth of mullite along its c-axis by coalescence of the surrounding fine grains to yield an anisotropic grain microstructure. At high seed concentration or at longer sintering time, the aspect ratio is limited by the impingement of the elongated grains and thickening occurs instead.

The mullite whiskers act as multiple nucleation sites for the diphasic precursor to form an 'overgrowth' layer. This overgrowth layer continues to grow with increasing temperature, resulting in highly anisotropic grains. Increasing the whisker concentration results in a gradual decrease in aspect ratio due to earlier impingement of the grains.

The boria-containing matrix enhances the mullite transformation kinetics and decreases the transformation temperature by 150°C compared with unseeded, undoped colloidal samples. The lower temperature appears to result from increased alumina solubility. By seeding with whiskers and doping with boria, highly anisotropic microstructures

consisting of anisotropic grains with lengths as long as 30 μm and aspect ratios as high as 10 were developed.

Acknowledgements

The authors gratefully acknowledge the support of the Office of Naval Research under grant number N00014-94-1-0007. One of us (W.C.) thanks the Cooperative Research Program of the Center for Advanced Materials at Penn State for support.

References

1. Aksay, I. A., Dabbs, D. M. & Sarikaya, M., Mullite for structural, electronic, and optical applications. *J. Am. Ceram. Soc.*, **74**(10) (1991) 2343–58.
2. Lessing, P. A., Gordon, R. S. & Mazdiyasni, K. S., Creep of polycrystalline mullite. *J. Am. Ceram. Soc.*, **58**(3–4) (1975) 149.
3. Prochazka, S. & Klug, F. J., Infrared-transparent mullite ceramic. *J. Am. Ceram. Soc.*, **66**(12) (1983) 874–80.
4. Yla-Jaaski, J & Nissen, H.-U., Investigation of superstructures in mullite by high resolution electron microscopy and electron diffraction. *Phys. Chem. Minerals*, **10** (1983) 47–54.
5. Pask, J. A., Zhang, X. W., Tomsia, A. P. & Yoldas, B. E., Effect of sol–gel mixing on mullite microstructure and phase equilibria in the α-Al_2O_3–SiO_2 system. *J. Am. Ceram. Soc.*, **70**(10) (1987) 704–7.
6. Von Lohre, W. & Urban, H., Contribution to the morphology of mullite. *Ber. Dtsch Keram. Ges.*, **37** (1960) 249–51.
7. Ismail, M. G. U., Arai, H., Nakai, Z. & Akiba, T., Mullite whiskers from precursor gel powders. *J. Am. Ceram. Soc.*, **73**(9) (1990) 2736–9.
8. Sacks, M. D. & Pask, J. A., Sintering of mullite-containing materials: I, effect of composition. *J. Am. Ceram. Soc.*, **6**(2) (1982) 65–70.
9. Perry, G. S., Microwave dielectric properties of mullite. *Trans. Brit. Ceram. Soc.*, **72** (1973) 279–83.
10. Ohashi, M., Tabata, H., Abe, O., Kanzaki, S., Mitachi, S. & Kumazawa, T., Preparation of translucent mullite ceramics. *J. Mater. Sci. Lett.*, **6** (1987) 528–30.
11. Huling, J. C. & Messing, G. L., Hybrid gels for homoepitactic nucleation of mullite. *J. Am. Ceram. Soc.*, **72**(9) (1989) 1725–9.
12. Mroz, T. J. & Laughner, J. W., Microstructures of mullite sintered from seeded sol–gels. *J. Am. Ceram. Soc.*, **72**(3) (1989) 508–9.
13. Horn, D. S. & Messing, G. L., Anisotropic grain growth in titania-doped alumina. *Mat. Sci. Eng. A.*, **A195** (1995) 169–78.
14. Fahrenholtz, W. G. & Smith, D. M., Densification and microstructure of sodium-doped colloidal mullite. *J. Am. Ceram. Soc.*, 77(5) (1994) 1377–80.
15. Sowman, H. G., Alumina–boria–silica ceramic fibers from the sol–gel process. In *Sol–Gel Technoloy for Thin Films, Fibers, Performs, Electronics, and Specialty Shapes*, ed. L. C. Klein, Noyes, Park Ridge, NJ, 1988, pp. 162–82.
16. Ihara, M., Imai, K., Fukunaga, J. & Yoshida, N., Crystal structure of boro-aluminate, $9Al_2O_3{\cdot}2SiO_2$. *Yogyo Kyokaishi*, **33**(2) (1980) 2605–9.
17. Richards, E. A., Goodbrake C. J. & Sowman, H. G., Reactions and microstructure development in mullite fibers. *J. Am. Ceram Soc.*, **74**(10) (1991) 2404–9.
18. Schneider, H. & Lipinski, T. R., Occurrence of pseudotetragonal mullite. *J. Am. Ceram. Soc.*, **71**(3) (1988) C-162–4.
19. Huling, J. C. & Messing, G. L., Epitactic nucleation of spinel in aluminosilicate gels and its effect on mullite cystallization. *J. Am. Ceram. Soc.*, **74**(10) (1991) 2374–81.
20. Wei, W.-C. & Halloran, J. W., Transformation kinetics of diphasic aluminosilicate gels. *J. Am. Ceram. Soc.*, **71**(1) (1988) 581–7.
21. Huling, J. C. & Messing, G. L., Hybrid gels designed for nucleation and crystallization control of mullite. In *Better Ceramics Through Chemistry IV (Materials Research Society Symposium Proceedings Vol. 180)*, eds B. J. J. Zelinski, C. J. Brinker, D. E. Clark & D. R. Ulrich, Materials Research Society, Pittsburgh, PA, 1990, pp. 515–26.
22. Sabol, S. M., Messing, G. L. & Tressler, R. E., Textured alumina fibers with elongated grains. *HiTemp Review 1992*, Vol. 1, NASA CP-10104, 21-1–14, 1992.
23. Wu, M. & Messing, G. L., Fabrication of oriented SiC whisker-reinforced mullite matrix composites by tape casting. *J. Am. Ceram. Soc.*, 77(10) (1994) 2586–92.